Available online at www.sciencedirect.com
SCIENCE DIRECT
ELSEVIER
Journal of Crystal Growth 291 (2006) 301–308
JOURNAL OF CRYSTAL GROWTH
www.elsevier.com/locate/jcrysgro

A study of the morphology of GaN seed layers on in situ deposited Si_xN_y and its effect on properties of overgrown GaN epilayers

Y.T. Moon[a,*], J. Xie[a], C. Liu[a], Y. Fu[a], X. Ni[a], N. Biyikli[a], K. Zhu[a], F. Yun[a], H. Morkoç[a], A. Sagar[b], R.M. Feenstra[b]

[a]*Department of Electrical and Computer Engineering, Virginia Commonwealth University, Richmond, VA 23284, USA*
[b]*Department of Physics, Carnegie Mellon University, Pittsburgh, PA 15213, USA*

Received 16 August 2005; received in revised form 19 January 2006; accepted 6 March 2006
Communicated by R.M. Biefeld

Abstract

We studied the morphological dependence of the initial GaN seed layers on in situ deposited Si_xN_y and its effect on the structural and electrical properties of GaN epilayers overgrown by low-pressure metalorganic chemical vapor deposition. Primarily scanning electron microscopy images were used for a systematic investigation of the effects of the growth parameters of Si_xN_y and GaN layers on the morphology of the initial GaN seed layers prior to overgrown layers. High-resolution X-ray diffraction measurements revealed that the full width at half maximum of (1 0 2) rocking curve decreased significantly from 8.4 to 4.6 arcmin as the chamber pressure was increased from 30 to 300 Torr for the growth of the 0.3 μm-thick initial GaN seed layer. Thermally activated carrier transport measurements in the overgrown GaN epilayers showed a V-shaped temperature-dependent electron concentration profile with a minimum at 80 K, the shape of which is attributed to a highly degenerate impurity band in the heavily silicon-doped GaN region at the GaN/Si_xN_y interface.

PACS: 81.15.Gh; 68.55.Jk; 68.37.Hk; 73.61.Ey

Keywords: A1. Morphology; A3. Metalorganic chemical vapor deposition; B1. Nitrides

1. Introduction

Recent advances in GaN-based semiconductor thin film technology have paved the way for high-power ultraviolet to visible light-emitting diodes, laser diodes, ultraviolet detectors, and field effect transistors. However, GaN-based semiconductors have a major drawback in terms of the lack of native substrates in large size and quantity [1]. High-performance GaN-based optoelectronic devices with high reliability critically require high material quality with low defect density. Currently, the best method to significantly reduce the threading dislocation (TD) density in GaN is the epitaxial lateral overgrowth (ELO) technique [2]. However, this method requires additional ex situ processes, resulting in high cost and reduced thermal conductivity due to the thick dielectric mask layer employed. Heretofore, a great deal of efforts with a variety of growth details all based on the ELO concept have been reported [3–8]. One of the most effective and practical methods is to employ in situ deposited Si_xN_y nanomasks [4,9–13]. Nanometer-thick Si_xN_y layers with a porous morphology can easily be prepared by simply flowing appropriately diluted silane for a short period on the substrate or the nitride film under the similar chamber ambient with that used for typical GaN growth. The premise of this method is to form GaN seeds on the template via the spontaneously formed open pores in the porous Si_xN_y layer followed by the growth emanating from the initial GaN seeds on the Si_xN_y nanomask. Thus, in order to maximize the efficacy of dislocation reduction, the precise control of the initial GaN seed layer is imperative. The caveat, as in the case of standard ELO, is that the Si_xN_y layer is expected to affect the electrical properties of the overgrown GaN epilayers by

*Corresponding author. Tel.: +1 804 440 6727; fax: +1 804 828 4269.
E-mail address: ymoon@vcu.edu (Y.T. Moon).

0022-0248/$ - see front matter © 2006 Elsevier B.V. All rights reserved.
doi:10.1016/j.jcrysgro.2006.03.010

Si diffusion. In this vein, we studied the parameters affecting the morphology of the initial GaN seed layers on in situ deposited Si_xN_y and the resultant structural and electrical properties of the overgrown GaN epilayers using low-pressure metalorganic chemical vapor deposition (MOCVD). In this paper, we report on the dependence of the morphology of the initial GaN seed layer on the growth parameters. Moreover, we also explore the influence of the seed layer on the crystalline quality of the overgrown GaN epilayers.

2. Experimental procedure

GaN epilayers were grown on n-type 6H SiC substrates in a low pressure MOCVD system. Trimethylgallium (TMGa), trimethylaluminum (TMAl), trimethylindium (TMIn), silane (SiH_4) and ammonia (NH_3) were used as sources of Ga, Al, In, Si and N, respectively. A 300 nm $Al_{0.26}Ga_{0.74}N$/100 nm AlN double buffer was employed for the GaN epilayer on SiC. A study of the initial GaN seed layers grown on in situ deposited Si_xN_y layers was performed using 2 μm GaN templates on sapphire. The growth details for the 2 μm GaN template on sapphire are described elsewhere [14]. The growth details of GaN on SiC are as follows: single-side polished 6H SiC (Si-face) substrates were annealed under flowing hydrogen at 1580 °C for 15 min in an inductively heated custom hydrogen annealing system to eliminate the damaged surface layer due to mechanical polishing. A 100 nm-thick AlN buffer layer was deposited at 1070 °C, 30 Torr with 10 μmol/min TMAl, 0.44 mol/min H_2, and 0.3 mmol/min NH_3. This was followed by the growth of a 300 nm-thick $Al_{0.26}Ga_{0.74}N$ at 1030 °C with 9.8 μmol/min TMAl, 40.2 μmol/min TMGa, and 89 mmol/min NH_3. Si_xN_y layers were deposited at 1020 °C, 200 Torr for 5 min by flowing 50 sccm of 100 ppm silane diluted in hydrogen. The 0.3 μm-thick initial GaN seed layers were grown on the Si_xN_y layer with a V/III ratio of 2000 at three different growth pressures of 30, 200, and 300 Torr. A 2 μm-thick GaN overgrowth was performed on the seed layer to attain coalesced surfaces at 1040 °C, 76 Torr with a V/III ratio of 4000 and 16 μmol/min TMIn as surfactant for improving structural properties. Finally, a nominally 1 μm-thick GaN was deposited to obtain atomically smooth epilayers at 1020 °C, 200 Torr with a V/III ratio of 4000. The surface morphology of the initial GaN seed layers and the overgrown GaN epilayers on the Si_xN_y was investigated using scanning electron microscopy (SEM). A high-resolution X-ray diffraction (XRD) system (X'Pert-MPD™, Philips) was used to examine the crystalline quality of GaN thin films. An atomic force microscope (AFM) (MultiMode™, Digital Instruments) was used in tapping mode to investigate the surface root mean square (rms) roughness of GaN. Temperature-dependent electrical properties of GaN on SiC were examined using a Hall effect measurement system (7504 HMS™, Lake Shore Cryotronics) in the van der Pauw configuration. Schottky diodes were fabricated to investigate electrical properties of GaN grown on SiC. Circular Au (100 nm) dots with a diameter of 300 μm formed the Schottky contacts while indium was used for the ohmic contacts. Current–voltage (I–V) and capacitance–voltage (C–V) measurements on Schottky diodes were performed at room temperature using a parameter analyzer (HP 4284A or a Keithley 4200).

3. Results and discussion

Fig. 1 displays a series of SEM images to illustrate the effect of Si_xN_y deposition conditions on the surface morphology of the overgrown 2 μm GaN. Fig. 1(a) shows randomly distributed, low density, large size polycrystalline GaN when 2% silane was used to deposit Si_xN_y for 10 min. This result demonstrates that there is no coherence between the overgrown GaN and the template due to the lack of open pores in the thick Si_xN_y. Fig. 1(b) shows well-aligned hexagonal GaN islands in the growth direction of c-axis when 250 ppm silane was introduced for 10 min. This result is indicative of the presence of open pores in a thinner Si_xN_y so that the pores could act as nucleation centers for GaN overgrowth. When silane was further diluted to 100 ppm and flowed for 5 min, partial coalescence of the overgrown GaN islands was observed as shown in Fig. 1(c). Fig. 1(d) shows the coalesced and flat surface morphology of a 2 μm GaN grown on the Si_xN_y deposited using 100 ppm silane for 2 min. It is reasonable to assume that as the exposed area of the underlying template increases by decreasing the Si_xN_y film thickness, the GaN nuclei during the initial stage of regrowth will be separated by smaller length scales of Si_xN_y, resulting in a rapid coalescence of overgrown GaN. In terms of the dislocation reduction efficacy, the rapid coalescence of regrown GaN is not desirable because a high density of initial GaN nuclei will: (i) increase the probability of threading dislocation penetration from the template into the overgrown GaN through the open pores; (ii) decrease the length of effective lateral overgrowth between initial GaN nuclei, and; (iii) increase grain boundaries in the coalesced overgrown GaN layer. Thus, in order to efficiently reduce the threading dislocation density in the overgrown GaN within a reasonable film thickness for practical device applications, we need to precisely control the properties of the initial GaN seed layers on the Si_xN_y. For further experiments in the realm of this study, a silane concentration of 100 ppm was used to deposit Si_xN_y layers with a deposition time of 5 min.

Fig. 2 shows the effect of the reactor pressure on the surface morphology for 0.5 μm-thick initial GaN seed layers grown on Si_xN_y with a V/III ratio of 2000 at 970 °C using 2 μm GaN templates. When the growth pressure of the initial GaN seed layer was 30 Torr, the surface almost coalesced with hexagonal pinholes formed during coalescence of the initial GaN islands [Fig. 2(a)]. When the growth pressure increased to 200 Torr, randomly distributed initial GaN seeds partially coalesced and had

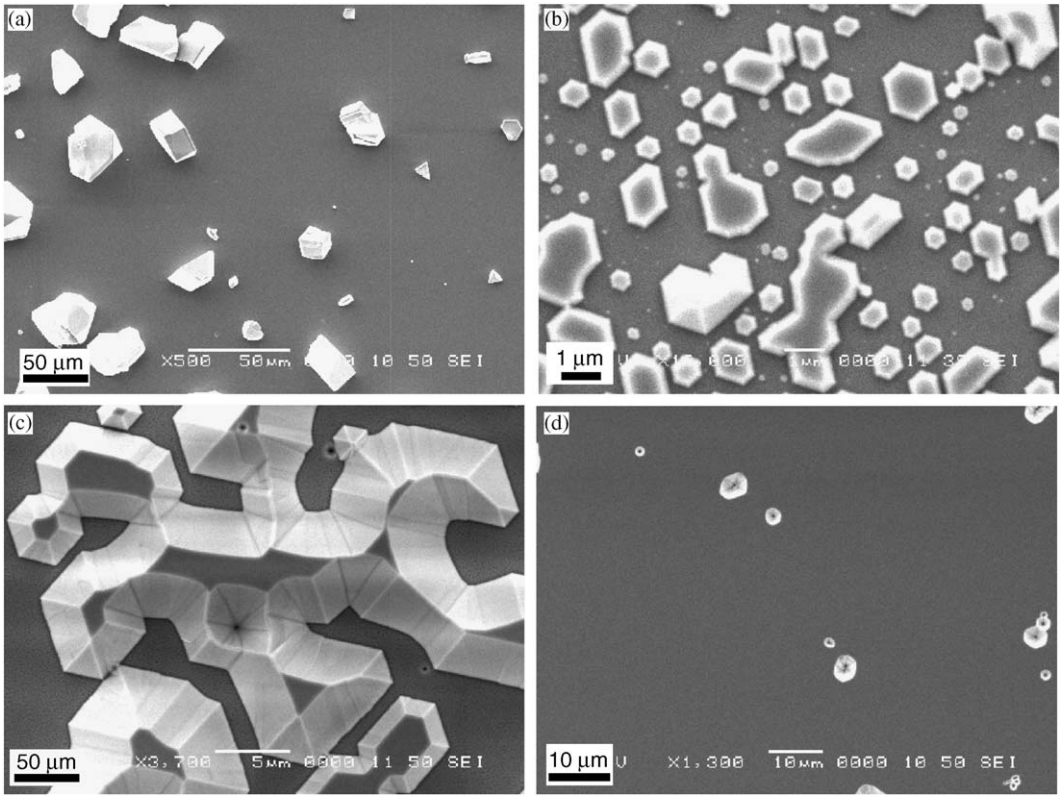

Fig. 1. The effects of silane density and deposition time on the SEM surface morphology of overgrown 2 μm GaN on the porous Si_xN_y thin films. (a) 2% silane for 10 min, (b) 250 ppm silane for 10 min (c), 100 ppm silane for 5 min, and (d) 100 ppm silane for 2 min with a flow rate of 50 sccm.

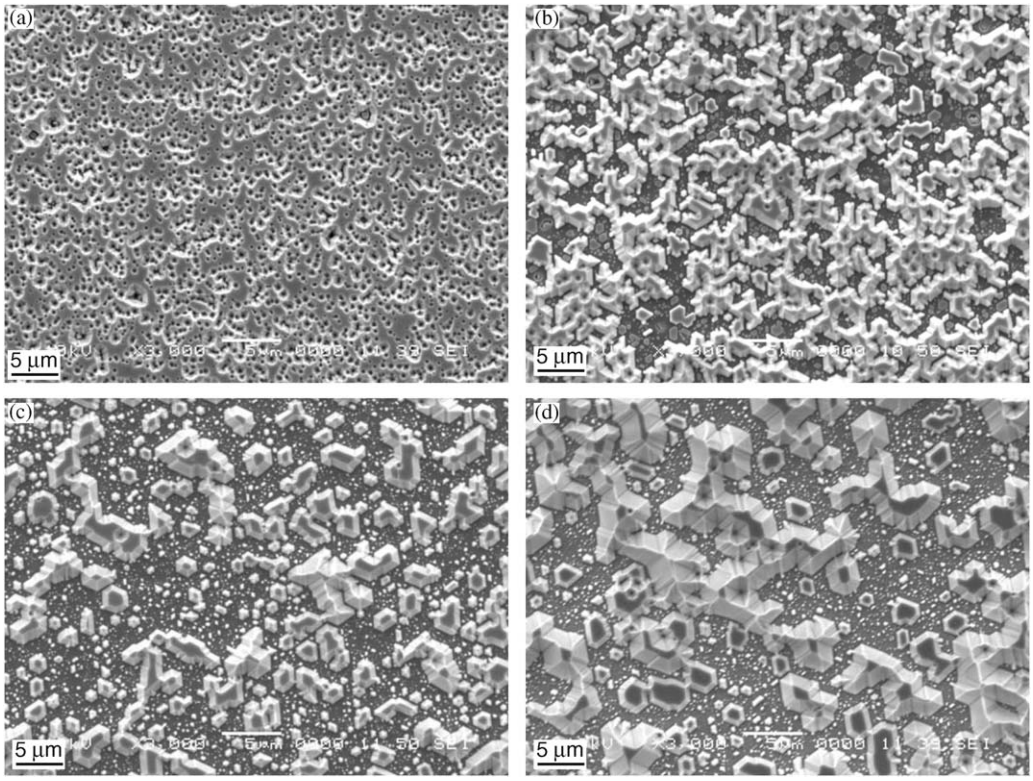

Fig. 2. The effects of growth pressure and layer thickness of initial GaN seed layers on the SEM surface morphology. (a) 30 Torr, 0.5 μm-thick, (b) 200 Torr, 0.5 μm-thick, (c) 300 Torr, 0.5 μm-thick, and (d) 300 Torr, 1 μm-thick. The seed layers were grown at 970 °C with a V/III ratio of 2000.

arbitrary shapes [Fig. 2(b)]. The initial GaN seeds became discontinuous and assumed a hexagonal shape when the growth pressure increased to 300 Torr [Fig. 2(c)]. Hexagonal facets of the initial GaN seeds at 300 Torr became obvious when the seed layer thickness increased to 1 μm [Fig. 1(d)]. It should be noted that in case of discontinuous GaN seeds, the overall seed layer thickness does not specify the average height of seeds and therefore we choose to report the deposition time. Fig. 2 illustrates that as the growth pressure of the initial GaN seed layer increases from 30 to 200, and then to 300 Torr, the density of GaN seeds decreased. In addition, the increase of the reactor pressure will enhance the development of thermodynamically stable crystallographic facets of wurtzite GaN seeds due to enhanced chemical etching by the hydrogen and ammonia gas mixture during growth.

The crystallographic facets of hexagonal GaN seeds grown at 200 and 300 Torr became obvious when the growth temperature increased from 970 to 1020 °C, as shown in Fig. 3(a) and (b), respectively. An increase of growth temperature will enhance the development of thermodynamically preferred crystallographic facets due to the enhancement of adatom surface diffusivity. An increase of growth temperature will also decrease the density of GaN seeds, the explanation of which is given below. Thermodynamically, it is expected that the atoms in relatively small GaN seeds will be more thermally unstable than those in large GaN seeds since small seeds have relatively large surface energy contribution to the total Gibbs free energy. Thus, when the growth temperature increases, the adatoms on relatively small GaN seeds will become more unstable than those on larger seeds. In addition, the diffusivity of mobile Ga atoms on the Si_xN_y surface will increase as the growth temperature increases. This will in turn cause mobile Ga atoms to thermodynamically prefer depositing on relatively large and stable GaN seeds formed on larger open pores in Si_xN_y. Consequently, an increase of growth temperature will retard the development of relatively small GaN seeds on smaller open pores, resulting in a decrease of the density of GaN islands. The density of GaN seeds grown at 200 Torr, 1020 °C further decreased when the V/III ratio increased from 2000 [Fig. 3(a)] to 4000 [Fig. 3(c)]. The hexagonal micro-facetted GaN pyramids which are uniformly distributed and well aligned on the Si_xN_y nanomask are beneficial for the reduction of threading dislocations when used as seeds for GaN regrowth [7,14]. But, large-sized micro-facetted GaN seeds with low density requires longer time to obtain coalesced and flat GaN surfaces with no appreciable surface undulations. Thus, an optimum thickness of the initial GaN seed layer needs to be determined, and another set of growth conditions which can enhance lateral overgrowth on the seed layer needs to be applied to attain a flat GaN surface with a reasonable film thickness. Further work in this study employed a seed layer thickness of 0.3 μm which produced a coalesced flat surface after

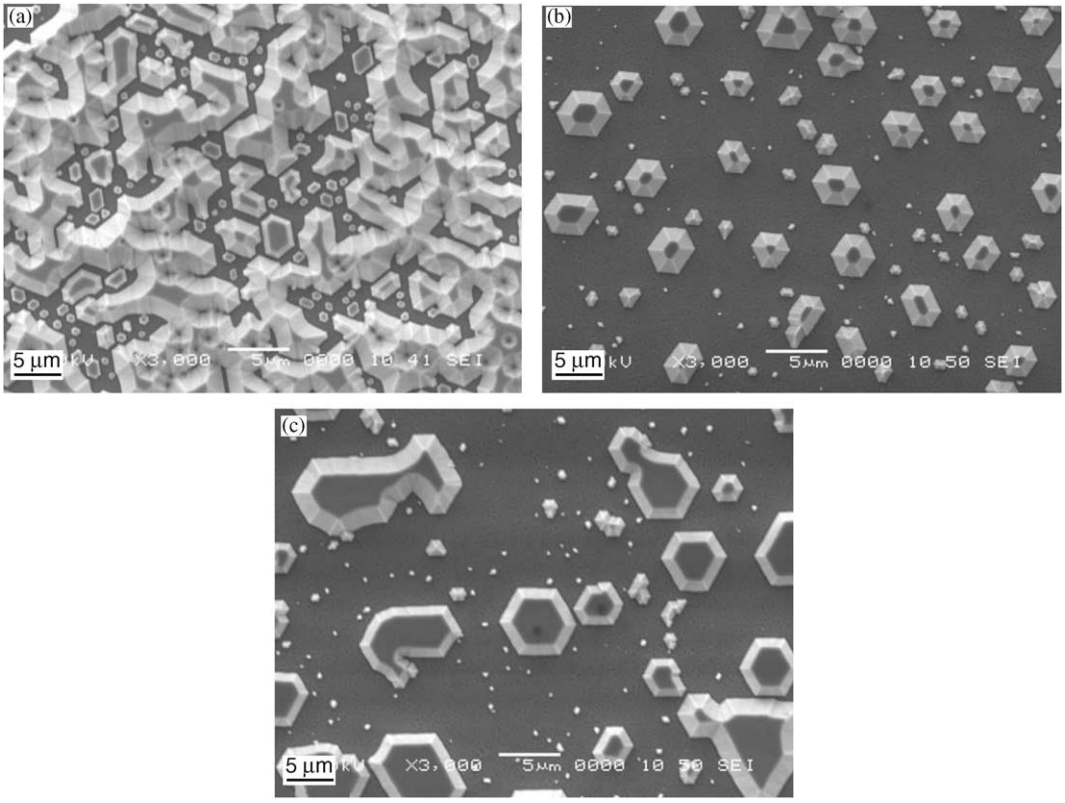

Fig. 3. The effects of growth pressure and V/III ratio of initial GaN seed layers on the SEM surface morphology. (a) 200 Torr, V/III 2000, (b) 300 Torr, V/III 2000, and (c) 200 Torr, V/III 4000. The 0.5 μm-thick seed layers were grown at 1020 °C.

2 μm regrowth. The desirable lateral epitaxial overgrowth conditions on the GaN seeds formed on a Si_xN_y layer will call for the enhancement of facet-controlled lateral overgrowth from the micro-facetted GaN seeds. Simultaneously, the formation of the small undesirable GaN clusters among the large hexagonal GaN islands during GaN overgrowth must be minimized in order to efficiently reduce the threading dislocation density in the overgrown GaN layer.

Based on the above study regarding the effects of growth parameters on the morphology of the initial GaN seed layer, three GaN epilayers were prepared on 6H SiC substrates using Si_xN_y. It is noted that GaN templates grown on sapphire instead of SiC substrates were used in the previous study due to the high cost of SiC. Different substrates may cause some difference. However, it is believed that the previous study is still meaningful because the morphology of the initial GaN seed layer was mainly influenced by the growth conditions of Si_xN_y and GaN seeds. The GaN epilayers were prepared to investigate the effect of growth pressure of the initial GaN seed layer on the structural and electrical properties of the GaN epilayers. As the growth pressure of 0.3 μm-thick initial GaN seed layer increased from 30 to 300 Torr, the full-width at half-maximum (FWHM) of the (102) XRD rocking curves decreased significantly from 8.4 to 4.6 arcmin (Table 1). This observation implies that the increase of growth pressure of GaN seed layer improves the crystalline quality of the overgrown 3 μm-thick GaN layer as a result of decreased threading dislocation density. This is further confirmed by a reduction in the leakage current density of Schottky diodes under reverse bias (Table 1). This is because the reverse leakage current can be related to electrically active threading dislocations, either by trapping impurities, carriers, and or point defects even if the dislocations by themselves do not have electrically active components [15].

The surface morphology of the three samples, A, B, and C listed in Table 1 was investigated using SEM measurements. Sample A with an initial GaN seed layer grown at 30 Torr showed surface crack lines which were absent in samples B and C. The formation of thermally induced surface cracks as observed on the GaN layer grown at 30 Torr was completely suppressed when a $20 \times$ (2 nmAlN/2 nmGaN) superlattice was inserted between the Si_xN_y and 100 nm AlN buffer in lieu of a 0.3 μm-thick $Al_{0.26}Ga_{0.74}N$ buffer layer.

The effect of the growth pressure of the initial GaN seed layer on the structural properties of the overgrown 3 μm-thick GaN epilayers was further investigated by wet chemical etching experiments for the overgrown GaN epilayers using molten KOH for 30 min. Figs. 4(a), (b) and (c) show the distribution of chemical etch pits of the 3 μm-thick GaN epilayers deposited on 0.3 μm-thick initial GaN seed layers grown at 30, 200 and 300 Torr, respectively. Fig. 4 clearly shows that as the growth pressure used for the initial GaN seed layer increased, the number of etch pits decreased and the laterally overgrown TD-free area increased. This observation can be understood in terms of the density of the initial GaN seeds. When the growth pressure for the initial GaN seed layer increases, the density of initial GaN islands decreases as discussed in relation to Fig. 2. This decrease results in a reduction of the probability of dislocation threading from the buffer layer toward the surface of the overgrown GaN epilayer through the GaN seeds formed on the open pores in the Si_xN_y layer. The decrease of density of GaN islands will also result in a reduction in the total area of grain boundaries which are formed during coalescence of GaN islands.

To study the electrical properties of GaN epilayers grown with the aid of Si_xN_y layers on 6H SiC substrates, samples B, C, tabulated in Table 1, and an n-type 6H SiC representing substrates used were analyzed by low-temperature Hall effect measurements in the van der Pauw configuration. Figs. 5(a) and (b) show the temperature-dependent sheet electron density and electron mobility profiles, respectively. It is noted that the temperature-dependent sheet electron density profiles of samples B and C show a density minimum at about 80 K while the electron density of n-type 6H SiC continuously decreases. (In case of 6H SiC, the data points below 60 K were not reliable due to the very high resistivity caused by carrier freeze-out.) It is expected that the electron transport in GaN samples grown on n-type SiC will take place through the GaN epilayer as well as through the conductive n-type substrate. But, conduction through these two layers alone cannot explain the high electron density below 80 K considering the carrier freeze-out particularly in bulk SiC and bulk GaN as donors are not very shallow. Thus, we need to consider the interfaces or the interlayers between the substrate and GaN epilayer to uncover the origin of the high electron density below 80 K. In order to investigate the conductivity of 300 nm $Al_{0.26}Ga_{0.74}N$/100 nm AlN double buffer layer in view of the consideration of

Table 1
The effect of growth pressure of 0.3 μm-thick initial GaN seed layer on the structural properties of overgrown 3 μm-thick GaN epilayers

Sample #	Seed growth pressure (Torr)	XRD rocking curve FWHM (arcmin)		Leakage current density at −10 V (A/cm^2)
		(0 0 2)	(1 0 2)	
A	30	7.0	8.4	1.8×10^{-2}
B	200	5.6	6.7	2.6×10^{-3}
C	300	4.7	4.6	4.1×10^{-4}

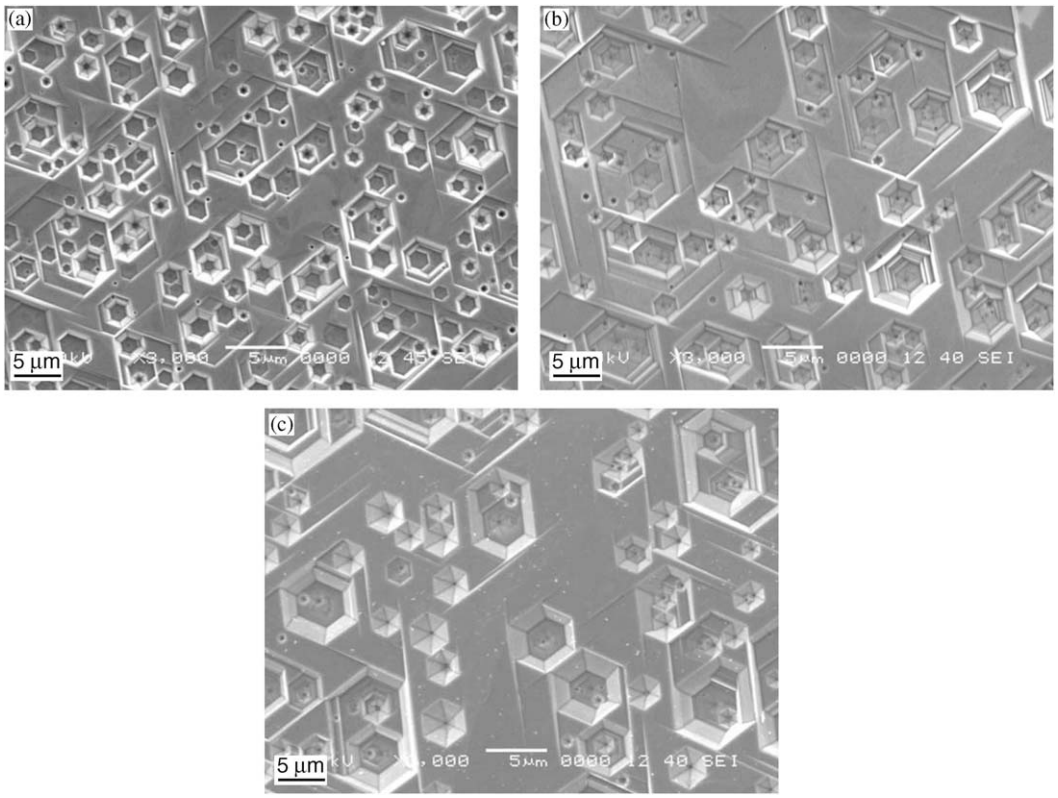

Fig. 4. The effect of growth pressure of initial GaN seed layer on the etch pit density of overgrown 3 μm-thick GaN epilayers. (a) 30 Torr, (b) 200 Torr, and (c) 300 Torr. The chemical wet etching was done in a molten KOH for 30 min.

polarization effects, the AlGaN/AlN double layer was deposited on *c*-plane sapphire. Interestingly, the AlN layer grown on sapphire at a high temperature showed crystalline quality comparable to that of AlN on SiC in terms of the (0 0 2) XRD rocking curve and a similar surface rms roughness of 0.3 nm. A room temperature Hall measurement of the AlGaN/AlN grown on sapphire showed insulating properties, which implies that the AlGaN/AlN double buffer layer is not responsible for the high electron density below 80 K in Fig. 5(a). The possibility of the existence of a two-dimensional carrier gas at the interface between the insulating AlN and carrier frozen SiC below 80 K can also be excluded by considering the mobility profiles in Fig. 5(b) which are dominated by ionized impurity scattering in the temperature range investigated.

The likely candidate for the origin of high electron density below 80 K may be related to the GaN/ Si_xN_y interface region. It is expected that the porous Si_xN_y layer will supply sufficient density of Si atoms to the bottom face of the overgrown GaN epilayer, which may result in formation of a degenerate impurity band. Furthermore, this kind of V-shaped carrier concentration profile has been observed in typical GaN thin films grown on *c*-plane sapphire substrates [16–18]. In case of GaN thin films grown on sapphire, the V-shape carrier concentration profile with a minimum at about 90 K has been attributed to a parallel conduction through the conduction band and a quasimetallic degenerate channel [16–21]. The conduction through the quasimetallic channel can be related to an impurity band in a highly defective GaN/sapphire interface region which is heavily doped by oxygen outdiffusion from the sapphire substrate [21,22]. In order to investigate the effect of Si diffusion from the Si_xN_y layer on the electron concentration profile of the overgrown GaN epilayer, *C–V* measurements were performed at room temperature using sample C in Table 1. In order to get reliable data from *C–V* measurements at a relatively high reverse bias, we selected sample C because the film quality was better than that of sample B. Fig. 6 shows the carrier concentration profile of sample C vs. depth calculated from the pertinent *C–V* profile. The inset of Fig. 6 shows the *C–V* profile up to −35 V. Part I of the carrier concentration profile in Fig. 6, which shows an average carrier concentration of $3 \times 10^{16}\,cm^{-3}$, corresponds to the top 1 μm-thick GaN layer grown using typical GaN growth conditions at 200 Torr. Parts II and III in the profile, which show a low carrier concentration of $6 \times 10^{14}\,cm^{-3}$, correspond to the laterally overgrown GaN on the initial GaN seed layer using growth conditions which can enhance lateral overgrowth at 76 Torr. The low carrier concentration of part II can be attributed to an increase of carbon incorporation efficiency due to the relatively low growth pressure of 76 Torr [23,24], which can be understood by considering that hydrogen etching effect for the removal of the acceptor

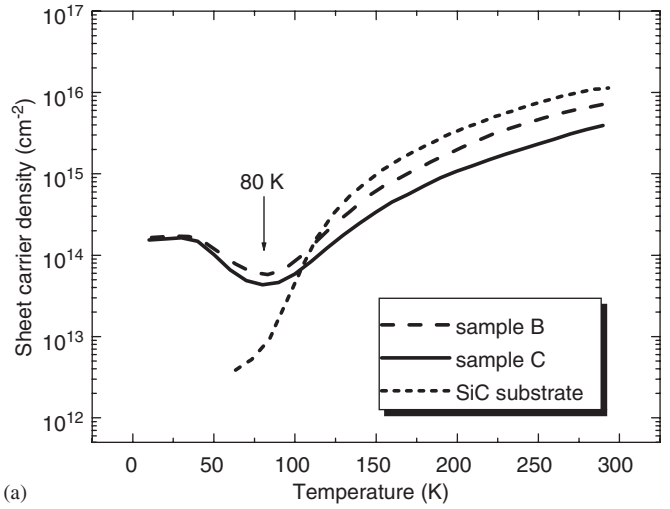

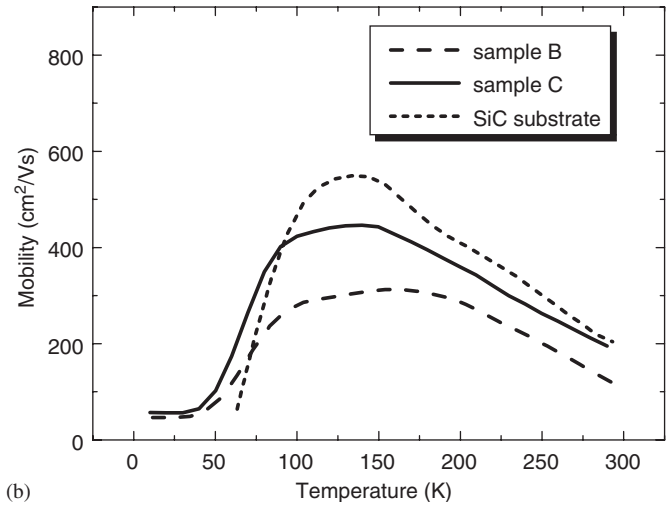

Fig. 5. The temperature-dependent (a) sheet electron density and (b) electron mobility profiles of samples B, C and the n-type 6H SiC substrate.

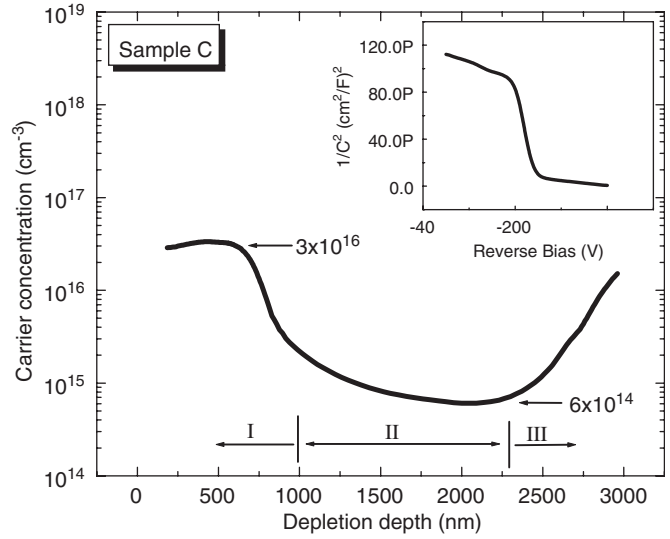

Fig. 6. The electron concentration profile of sample C along the depth which was calculated from a *C–V* profile. The inset of Fig. 6 shows the *C–V* profile down to −35 V.

impurities from the dissociation of $Ga(CH_3)_3$ source molecules on the growing GaN surface will decrease as the chamber pressure decreases by decreasing the effective number of hydrogen molecules remaining in the chamber. It is noteworthy that the carrier concentration in part III increased toward the Si_xN_y layer. The increase of carrier concentration can be attributed to the apparent Si diffusion up to about 0.7 μm from the interface between the overgrown GaN and Si_xN_y layers. The diffusion of Si from Si_xN_y was further confirmed by a secondary ion mass spectrometry analysis (not shown here). This result implies that the interface side of overgrown GaN on the Si_xN_y layer is heavily silicon doped, resulting in a formation of a highly degenerate impurity band. Thus, it is believed that the high electron density below 80 K in Fig. 5 (a) is due to a highly degenerate impurity band in the heavily silicon doped GaN region at the GaN/ Si_xN_y interface. Additionally, we prepared a controlled GaN epilayer grown without using the Si_xN_y interlayer to compare the electrical properties of GaN epilayers. However, we could not obtain reliable electrical properties of the controlled sample due to severe film cracking. Recently, Ive et al. [25] observed a metallic-like conductivity at 77 K in heavily Si-doped ($[Si] = 1-2 \times 10^{19}\ cm^{-3}$) AlN/GaN multiple layers grown on a conductive SiC but not in undoped layers, which further supports our conclusion.

4. Conclusions

We investigated the effects of growth parameters on the surface morphology of the initial GaN seed layers. The control of the growth parameters paved the way for attaining an optimum surface morphology of the initial GaN seed layer and produced micro-facetted hexagonal GaN islands. As the growth pressure of 0.3 μm-thick initial GaN seed layer increased from 30 to 300 Torr, the crystalline quality of 3 μm-thick overgrown GaN epilayer improved significantly by presumably a reduction of threading dislocation density, as determined from the asymmetric X-ray data. The electronic conduction through the overgrown GaN epilayers was investigated by temperature-dependent Hall effect measurements. A thermally activated electronic conduction of the overgrown GaN epilayers showed a V-shaped temperature-dependent electron concentration profile with a minimum at 80 K. The V-shaped carrier profile is attributed to the existence of a highly degenerate impurity band in the silicon-doped GaN region at the GaN/Si_xN_y interface.

Acknowledgments

This work was supported by a grant from ONR (Dr. C. E. C. Wood). The authors acknowledge collaboration and discussion with Prof. T. S. Kuan during the early stage of this work.

References

[1] H. Morkoç, Nitride Semiconductors and Devices, Springer, Berlin, 1999 (second and expanded edition in process).
[2] O.H. Nam, M.D. Bremser, T.S. Zheleva, R.F. Davis, Appl. Phys. Lett. 71 (1997) 2638.
[3] P. Gibart, Rep. Prog. Phys. 67 (2004) 667.
[4] S. Haffouz, H. Lahrèche, P. Vennéguès, B. Beaumont, F. Omnès, P. Gibart, Appl. Phys. Lett. 73 (1998) 1278.
[5] T. Akasaka, Y. Kobayashi, S. Ando, N. Kobayashi, Appl. Phys. Lett. 71 (1997) 2196.
[6] B. Beaumont, V. Bousquet, P. Vennéguès, M. Vaille, A. Bouillé, P. Gibart, S. Dassonneville, A. Amokrane, B. Sieber, Phys. Stat. Sol. (a) 176 (1999) 567.
[7] K. Hiramatsu, K. Nishiyama, M. Onishi, H. Mizutani, M. Narukawa, A. Motogaito, H. Miyake, Y. Iyechika, T. Maeda, J. Crystal Growth 221 (2000) 316.
[8] I. Kidoguchi, A. Ishibashi, G. Sugahara, Y. Ban, Appl. Phys. Lett. 76 (2000) 3768.
[9] S. Sakai, T. Wang, Y. Morishima, Y. Naoi, J. Crystal Growth 221 (2000) 334.
[10] A. Dadgar, M. Poschenrieder, A. Reiher, J. Bläsing, J. Christen, A. Krtschil, T. Finger, T. Hempel, A. Diez, A. Krost, Appl. Phys. Lett. 82 (2003) 28.
[11] X.L. Fang, Y.Q. Wang, H. Meidia, S. Mahajan, Appl. Phys. Lett. 84 (2004) 484.
[12] K. Pakuła, R. Bożek, J.M. Baranowski, J. Jasinski, Z. Liliental-Weber, J. Crystal Growth 267 (2004) 1.
[13] A. Sagar, R.M. Feenstra, C.K. Inoki, T.S. Kuan, Y. Fu, Y.T. Moon, F. Yun, H. Morkoç, Phys. Stat. Sol. (a) 202 (2005) 722.
[14] Y.T. Moon, Y. Fu, F. Yun, S. Dogan, M. Mikkelson, D. Johnstone, H. Morkoç, Phys. Stat. Sol. (a) 202 (2005) 718.
[15] E.J. Miller, E.T. Yu, P. Waltereit, J.S. Speck, Appl. Phys. Lett. 84 (2004) 535.
[16] J.J. Harris, K.J. Lee, I. Harrison, L.B. Flannery, D. Korakakis, T. Cheng, C.T. Foxon, Z. Bougrioua, I. Moerman, W. Van der Stricht, E.J. Thrush, B. Hamilton, K. Ferhah, Phys. Stat. Sol. (a) 176 (1999) 363.
[17] D.C. Look, D.C. Reynolds, J.W. Hemsky, J.R. Sizelove, R.L. Jones, R.J. Molnar, Phys. Rev. Lett. 79 (1997) 2273.
[18] R. Molnar, T. Lei, T.D. Moustakas, Appl. Phys. Lett. 62 (1993) 72.
[19] D.C. Look, J.R. Sizelove, Phys. Rev. Lett. 82 (1999) 1237.
[20] B.J. Ansell, I. Harrison, C.T. Foxon, J.J. Harris, T.S. Cheng, Electron. Lett. 36 (2000) 1237.
[21] C. Mavroidis, J.J. Harris, M.J. Kappers, N. Sharma, C.J. Humphreys, E.J. Thrush, Appl. Phys. Lett. 79 (2001) 1121.
[22] G. Popovici, W. Kim, A. Botchkarev, H. Tang, J. Solomon, H. Morkoç, Appl. Phys. Lett. 71 (1997) 3385.
[23] G. Parrish, S. Keller, S.P. DenBaars, U.K. Mihsra, J. Electron. Mater. 29 (2000) 15.
[24] A. Armstrong, A.R. Arehart, B. Moran, S.P. DenBaars, U.K. Mishra, J.S. Speck, S.A. Ringel, Appl. Phys. Lett. 84 (2004) 374.
[25] T. Ive, O. Brandt, K.H. Ploog, J. Crystal Growth 278 (2005) 355.